MESH MOTION METHODS FOR NUMERICAL AERODYNAMIC DESIGN OF LIFT AND CONTROL SURFACES

Introduction

This work is part of great effort to build a numerical platform to simulate and optimize fluid-structure interaction problems applied to the design of UAVs. The creation of a numerical analysis tool to design lift and control surfaces depends on the development of specific knowledge in moving mesh strategies and data interpolation methods between mesh domains. In order to create this modular numerical platform for the solution of fluid-structure interaction problems, several moving mesh methods were implemented and tested in a scientific CFD code based on a finite element projection method and a performance comparison was done resulting on the definition of the best moving mesh strategies.

Traditionally, the movement of numerical meshes related to fluid domains due to the displacement of the boundary between fluid and structure is done by solving a pseudo-elastic problem referent to the fluid mesh. The first numerical schemes (Batina, 1990, Johnson & Tezduyar, 1994) to solve the mesh motion problem transformed the fluid mesh into a fictitious structure where lineal springs were placed between the mesh element nodes. The stiffness of every lineal spring is inversely proportional to the distance between nodes. The total stiffness of the pseudo structure has the contribution of the stiffness of each lineal spring. Therefore, the finte element method was the natural choice for solving the mesh motion problem. However, this procedure was limited to problems with small mesh deformations because of the possibility of collapsing the elements.

A more complete approach uses the superposition of lineal and torsional springs (Farhat et al., 1998). Similarly to lineal spring, the stiffness of the torsional springs is proportional to the inverse of the angle in radians between to edges connected to each element node, the vertex of the element. From the beginning the linear and torsional spring method was developed for two-dimensional triangular elements. The adaptation of technique to three-dimensional elements such as tetrahedrons required a modification in the position of the torsional spring action plane. For three-dimensional elements it was necessary to avoid not only the collapse of the face of the element but also the volume of the element (Degand and Farhat, 2002). One of the difficulties faced by this method is to guarantee the mesh quality. Despite of preventing issues with collapsed elements, the moving mesh may have regions with elements that are excessively stretched or squeezed.

The most recent approach for moving meshes was developed for the solution of fluid-interaction problems using the open source code based on finite

volumes called OpenFOAM (Jasak and Tukovic, 2007). The displacement field of the mesh is obtained by the solution of a diffusion problem that propagates the displacement of the fluid-structure boundary to the interior of the fluid domain. The displacement computation is now associated to the velocity of modification of the mesh, or the nodal velocity field. The formulation of the problem is based on application of the Laplace operator to the nodal velocity field. The Laplace equation is solved by a finite element method, given the nodal velocity at the fluid-structure boundary. The mesh displacement is recovered multiplying the velocity by a predefined time step. The main drawback of this method is the choice of the diffusivity coefficient to avoid collapsed elements in the moving mesh process.

The idea of using the nodal velocity field to solve the mesh motion problem is not new (Lohner and Yang, 1996). One could interpret it as a particular case of a pseudo flow problem, more specifically a pseudo-Stokes problem. The advantage of modeling the mesh motion problem by using Stokes flow equations is possibility of getting a final mesh configuration with better element quality. The constraint of divergence null may guarantee the mesh quality by avoiding collapsed elements and the smoothness of the solution would improve excessively distorted elements. The main difficulties of this methodology is also in the choice of an adequate diffusion coefficient and because the solution of a flow problem is a time consuming process. The efficiency of the flow problem solution can be improved by using a projection finite element method as solver.

In this work several methods based on the pseudo structure and pseudo flow field strategies are implemented and tested. The methods are: Laplacian operator, Lineal spring analogy, Torsional spring analogy, Lineal-Torsional spring analogy and Pseudo-Stokes problem. The performance of the different methods is accessed by solving the moving mesh problem of a rotating rigid airfoil with a prescribed constant rotation velocity.

The structure of this paper is divided in five sections, including section 1 for the introduction. In section 2, the mesh motion strategies are introduced, basically two strategies are explored, one consider the mesh as a pseudo structure and the other as a pseudo flow field. The section 3 presents a summary of the numerical methods used to solve the mesh motion strategies proposed. In section 4, a specific rule is introduced to evaluate the mesh quality during the moving mesh process, and to illustrate this concept, the results of the solution of a rotating rigid airfoil obtained by several moving mesh methods are presented. In addition, results of the numerical simulation of a laminar flow over a rotating airfoil are also introduced to evaluate the mesh motion technique. Finally, section 5 presents the main conclusions of this work.

Mesh Motion Strategy

There exists two main strategies to move mesh grids in numerical simulations of fluid-structure interaction problems, one is to consider the mesh as a pseudo structure or a second option is to consider the mesh as a pseudo flow field. For the first strategy the mesh motion problem is modeled as a dynamic system with prescribed displacement boundary conditions. The final mesh configuration is determined by solving the dynamic equation of a pseudo-structural problem for its displacement field that is added to the previous mesh configuration. The second strategy consists in modeling the mesh motion problem as pseudo fluid problem. The final mesh configuration is computed by solving the governing equation of a pseudo flow problem for its velocity field which is converted into displacement using a time increment and added to a previous mesh configuration.

Pseudo structure strategy

The dynamic governing equation for a continuous pseudo-structural system (Farhat et al., 1998) is represented as described in:

$$\rho_{ps}\frac{\partial^2 \mathbf{x}}{\partial t^2}+\nabla.\boldsymbol{\sigma}_{ps}\left(\boldsymbol{\varepsilon}_{ps}\left(\mathbf{x}\right),\frac{\partial \boldsymbol{\varepsilon}_{ps}\left(\mathbf{x}\right)}{\partial t}\right)=\mathbf{f}_{ps} \tag{1}$$

$$\mathbf{x}\left(t\right)=\hat{\mathbf{x}}\left(t\right)\ \text{on}\ \Gamma_{ps} \tag{2}$$

where $\mathbf{x}\left(t\right)$ is the time dependent vector of the mesh position, ρ_{ps} is the pseudo-structural density, $\boldsymbol{\sigma}_{ps}$ e $\boldsymbol{\varepsilon}_{ps}$ are the pseudo-structural stress and strain tensors, respectively, $\mathbf{f}_{ps}$ is the vector of reaction forces acting on the domain and $\hat{\mathbf{x}}$ are the values of the mesh position on the fictitious structure boundary Γ_{ps}.

Pseudo flow field strategy

By considering a time dependent laminar and incompressible pseudo flow problem, the mesh motion governing equation is described as:

$$\nabla.\mathbf{u}=0 \tag{3}$$

$$\frac{\partial^2 \mathbf{u}}{\partial t^2}+\left(\nabla\mathbf{u}\right)\mathbf{u}=-\frac{1}{\rho_{pf}}\nabla p+\nabla.\left(\nu_{pf}\nabla\mathbf{u}\right)+\mathbf{f}_{pf} \tag{4}$$

where $\mathbf{u}(\mathbf{x},t)$ e $p(\mathbf{x},t)$ represent, respectively, the velocity and the pressure fields of the pseudo flow, ρ_{pf} and ν_{pf} are in this order the density and the viscosity of the pseudo fluid problem and $\mathbf{f}_{pf}$ is a given force function. One of the advantages of the pseudo flow modeling strategy is the constraint imposed by the divergent of the velocity field to be null that has an impact in the preservation of the mesh quality over the mesh motion process. The boundary conditions are defined on $\Gamma_{pf} = \Gamma_d \cup \Gamma_m \cup \Gamma_o$ by:

$$\mathbf{u}(\mathbf{x},t) = \mathbf{u}_d \text{ on } \quad \Gamma_d \tag{5}$$

$$\mathbf{u}(\mathbf{x},t) = \mathbf{v} \text{ on } \Gamma_m \tag{6}$$

$$p(\mathbf{x},t) = p_{ref} \text{ on } \Gamma_o \tag{7}$$

The subset Γ_d represents the boundary values that are constant where the Dirichlet boundary condition for the velocity field is prescribed. Γ_m is the moving boundary, where the fluid velocity is equivalent to the domain velocity. Γ_o is the outlet boundary condition where a reference pressure is prescribed.

An alternative to build the governing equation to model the mesh motion problem is to only consider the diffusive part of the Eq. (4) resulting in the Laplace equation (Jasak and Tukovic, 2007).

$$\nabla.\left(\nu_{pf}\nabla\mathbf{u}\right) = 0 \tag{8}$$

The drawback of the Laplace equation is that the largest mesh movement happens close to the moving boundary, potentially leading to local deterioration of the mesh quality. This problem is avoided by employing a variable diffusivity (ν_{pf}), what may confine the largest deformation to the internal part of the mesh.

Numerical Solution Methodology

Pseudo structure solution

The governing equation of the motion of the mesh on its discrete form is built considering the mesh as a pseudo-elastic structure (Batina, 1991, Koobus et al., 1998, Degand and Farhat, 2002):

$$\bar{\mathbf{M}}\ddot{\boldsymbol{\chi}} + \bar{\mathbf{C}}\dot{\boldsymbol{\chi}} + \bar{\mathbf{K}}\boldsymbol{\chi} = \bar{\mathbf{R}} \tag{9}$$

where $\boldsymbol{\chi}$ is the vector of mesh displacement, $\bar{\mathbf{M}}$, $\bar{\mathbf{C}}$ and $\bar{\mathbf{K}}$ are respectively the fictitious mass, damping and stiffness matrices associated to the fluid grid and

$\bar{\mathbf{R}}$ is the reaction force. The first and second time derivatives are represented in this order by the dot signs ($\dot{}$) and ($\ddot{}$). For a quasi-static model the fictitious mass and damping matrices are neglected (Farhat et al., 1998), resulting in

$$\bar{\mathbf{K}}\boldsymbol{\chi} = \bar{\mathbf{R}} \tag{10}$$

The quasi-static approach, due to its simplified structure and solution strategy, is usually preferred for the modeling of fluid-structure interaction problems. The quasi-static fluid mesh motion equations obey the kinematic compatibility between fluid and structure. The kinematic compatibility dictates how the position $\boldsymbol{\chi}_{\Gamma_{ps}}$ of mesh on the moving boundary Γ_{ps} is related to the mesh boundary velocity $\mathbf{u}_{\Gamma_{ps}}^{n+1}$ at the referent time step by:

$$\boldsymbol{\chi}_{\Gamma_{ps}} = \Delta t \, \mathbf{u}_{\Gamma_{ps}}^{n+1} \tag{11}$$

where Δt is the problem time step. For this work the mesh boundary points have a uniform rotation movement of radius $\mathbf{r}$ with respect to a specified center point. Therefore, the boundary moves as if there was a rigid structure rotating with a constant angular velocity ω.

$$\mathbf{u}_{\Gamma_{ps}}^{n+1} = \mathbf{r}\,\omega \tag{12}$$

The fictitious stiffness matrix $\bar{\mathbf{K}}$ and the reaction force vector $\bar{\mathbf{R}}$ in equation can be divided in subsets related to the internal (Ω_{ps}) and external (Γ_{ps}) degrees of freedom of the fluid mesh.

$$\begin{bmatrix} \bar{\mathbf{K}}_{\Omega_{ps}\Omega_{ps}} & \bar{\mathbf{K}}_{\Omega_{ps}\Gamma_{ps}} \\ \bar{\mathbf{K}}_{\Omega_{ps}\Gamma_{ps}} & \bar{\mathbf{K}}_{\Gamma_{ps}\Gamma_{ps}} \end{bmatrix} \begin{bmatrix} \boldsymbol{\chi}_{\Omega_{ps}} \\ \boldsymbol{\chi}_{\Gamma_{ps}} \end{bmatrix} = \begin{bmatrix} \bar{\mathbf{R}}_{\Omega_{ps}} \\ \bar{\mathbf{R}}_{\Gamma_{ps}} \end{bmatrix} \tag{13}$$

Equation (13) is solved with the condition of null force on the internal grid points ($\bar{\mathbf{R}}_{\Omega_{ps}} = 0$). Also, in this work for the mesh motion problem, a quasi-static model is used as described in Eq. (10), and the fictitious stiffness matrix $\bar{\mathbf{K}}$ is constructed by improved spring analogy methods (Koobus et al., 1998, Farhat et al., 1998, Degand and Farhat, 2002). Three methods based on the pseudo structural approach are tested: a lineal spring method, a torsinal spring method and lineal-torsional spring method.

As the main goal is to deal with fluid-structure interaction problems of small to medium scale, the solution strategy employs a direct method to solve the mesh motion linear system of equations. The direct method is preferred

because of its simplicity and robustness. The mesh position $\mathbf{x}^{n+1}$ is updated by summing the mesh displacement vector to the previous configuration of the mesh position vector $\mathbf{x}^{n}$, such as follows:

$$\mathbf{x}^{n+1} = \mathbf{x}^{n} + \begin{bmatrix} \chi_{\Omega_{ps}} \\ \chi_{\Gamma_{ps}} \end{bmatrix} \tag{14}$$

Pseudo flow solution

The following methodology is based on the semi-explicit iterative solution of the systems of equations (3)-(4) after a time and a spatial discretization, and considering a projection method framework (Goldberg and Ruas, 1999, Guermond et al., 2006, Lohner et al., 2006).

For a given $\Delta t > 0$ and considering the set of variables $\mathbf{u}^{n}$, p^{n} and $\mathbf{x}^{n}$ known from the previous time step t. The solution $\mathbf{u}^{n+1}$, p^{n+1} and $\mathbf{x}^{n+1}$ at the time $t + \Delta t$ is computed by using a staggered approach such as:

$$\frac{1}{\Delta t}\left(\mathbf{u}^{*} - \mathbf{u}^{n}\right) = -\frac{1}{\rho_{pf}}\nabla p^{n} + \nabla.\left(\nu_{pf}^{n}\nabla\mathbf{u}^{n}\right) + \mathbf{f}_{pf} \tag{15}$$

$$\frac{1}{\Delta t}\left(\mathbf{u}^{n+1} - \mathbf{u}^{*}\right) = -\frac{1}{\rho_{pf}}\nabla\left(p^{n+1} - p^{n}\right) \tag{16}$$

$$\nabla.\mathbf{u}^{n+1} = 0 \tag{17}$$

In Eq. (15) the convective term is neglected highlighting the use of a Pseudo-Stokes formulation to model the mesh motion problem. The fractional step method introduces a predicted velocity $\mathbf{u}^{*}$ which is corrected at the end of the block. Also, taking the divergence of the Eq. (16) and using Eq. (15) the Poisson equation is obtained:

$$\nabla^{2}\left(p^{n+1} - p^{n}\right) = \frac{\rho_{pf}}{\Delta t}\nabla.\mathbf{u}^{*} \tag{18}$$

and the boundary condition for Eq. (18) is:

$$\nabla^{2}\left(p^{n+1} - p^{n}\right).\mathbf{n} = \frac{\rho_{pf}}{\Delta t}\nabla.\mathbf{u}^{*}.\mathbf{n} \quad \text{on } \Gamma_{pf} \tag{19}$$

The projection method here described is called Incremental Projection Scheme. This method is a modification of the version proposed by Chorin (1968) which improves convergence as reported in the literature (Codina and Blasco, 2000, Codina, 2000, Guermond et al., 2006).

By considering the dimension of the finite element space equals to N and defining the base function as $\{\mathbf{N}_i : i = 1, \ldots, N\}$ and $\{\mathbf{N}_j : j = 1, \ldots, N\}$. The matrix form of the discrete finite element problem is:

Step 1: Predict velocity through the Momentum equation

$$\mathbf{M}\,\Delta\mathbf{u}^{*} = \mathbf{F}_{\mathbf{u}}^{*}\left(\mathbf{u}^{n}, p^{n}, \mathbf{x}^{n}\right) \tag{20}$$

Step 2: Poisson problem

$$\mathbf{A}\,\Delta p^{n+1} = \mathbf{F}_{p}^{*}\left(\mathbf{u}^{*}, \mathbf{x}^{n}\right) \tag{21}$$

Step 3: Velocity correction – projection on the divergence free space

$$\mathbf{M}\,\Delta\mathbf{u}^{n+1} = \mathbf{F}_{\mathbf{u}}\left(p^{n+1}, \mathbf{x}^{n}\right) \tag{22}$$

Step 4: Update the mesh position

$$\mathbf{x}^{n+1} = \mathbf{x}^{n} + \mathbf{u}^{n+1}\,\Delta t \tag{23}$$

Similarly to what is established to the pseudo structural methodology, the moving boundary Γ_m rotates with a constant angular velocity ω as if it was a rigid structure.

$$\mathbf{v} = \mathbf{r}\,\omega \tag{24}$$

For equations (20) to (22), $\mathbf{M}$ and $\mathbf{A}$ are the mass and the Laplacian matrices which are given by:

$$\mathbf{M}_{ij} = \frac{1}{\Delta t}\left(\mathbf{N}_i, \mathbf{N}_j\right) \tag{25}$$

$$\mathbf{A}_{ij} = \left(\nabla\mathbf{N}_i, \nabla\mathbf{N}_j\right) \tag{26}$$

The vectors $\mathbf{F}_{\mathbf{u}}^{*}$, $\mathbf{F}_p$ and $\mathbf{F}_{\mathbf{u}}$ are related to the discretization of the right-hand side of the equations through steps 1 to 3, and the boundary integral terms referent to the boundary conditions are also included to these vectors.

The greatest advantage of presented numerical scheme at the steps 1 to 3 is the mass matrix. In order to enhance convergence and time efficiency the mass matrix is lumped in a diagonal form, and its construction is performed only when the mesh position is updated. As for the Laplacian operator which symmetric, Eq. (21) is solved by a preconditioned conjugated gradient method (PCG) using a partial Cholesky factorization as preconditioner. For the numerical scheme, the time step computation or definition is directly linked to the viscosity term ν_{pf} and vice-versa (Massarotti et al., 2006).

The numerical scheme for particular case that employs the Laplacian equation to solve the mesh motion problem is represented as follows

$$\mathbf{M}\,\Delta\mathbf{u}^{n+1} = \mathbf{F}_{\mathbf{v}}\left(\mathbf{v}, \mathbf{x}^{n}\right) \tag{27}$$

where $\mathbf{F}_{\mathbf{v}}$ is the right-hand side resulting from the application of the boundary conditions to the Laplacian equation (Jasak and Tukovic, 2007). Also, the mesh update is performed as showed in Eq. (23).

Numerical Results

Mesh motion methods evaluation

The meshing process is defined as the breaking of any given domain into smaller elements. This division aims to facilitate the numerical solving of differential equations at this domain by replacing that equation into a set of algebraic equations. Those elements can be triangles or rectangles (for a 2D case) or tetrahedral or hexahedra elements. It is an important part of pre-processing, thus the demand for mesh generators that has improved robustness, speed and quality is very high, and since a low quality mesh can lead to inconsistent results. This care on meshing is more necessary when one turns its attention to simulation with moving boundaries that use mesh deformation. It is necessary to guarantee that the mesh elements hold a minimal of their quality after the deformation process, in order to do not affect the quality of the solution and the time needed to obtain it. So, a mesh quality evaluation method must be implemented to assess the quality of every element, as well as how suitable a particular meshing is for the analysis type. The present paper will use the work of Rypl (1998), that consist in evaluate the element quality with respect to the equilateral simplex (as the best possible element), Noleto, Barcelos e Brasil Junior (2009). For a 2D triangular element, the quality is expressed as:

$$q = f\frac{A}{a^2 + b^2 + c^2} \tag{28}$$

where A is the area, a, b and c are the lengths of the element´s sides and $f = 4/\sqrt{3}$ is a normalizing factor which justifies the quality of an equilateral triangle to 1. This parameter is calculated for every element. It is important to indicate how values of q are adequate to ensure a geometric topology that leads to an accurate calculation. Extremely deformed elements can lead to inaccurate calculations, and the solution robustness will be severely affected by this geometry aspect, as well as the convergence. Based on that, an important conclusion can be affirmed: if the quality drops to very small values after the deformation, than the calculation will be compromised by the element geometry shape. Therefore, it is reasonable to assume that quality values between 1 and 0.5 are values that will maintain, or will not extremely affect, the calculation. Values below 0.5 indicates that the mesh quality can influence the calculation for the worse, and far small values of q indicates that the element is highly

distorted, which will lead to poor results and affect the calculation robustness and convergence.

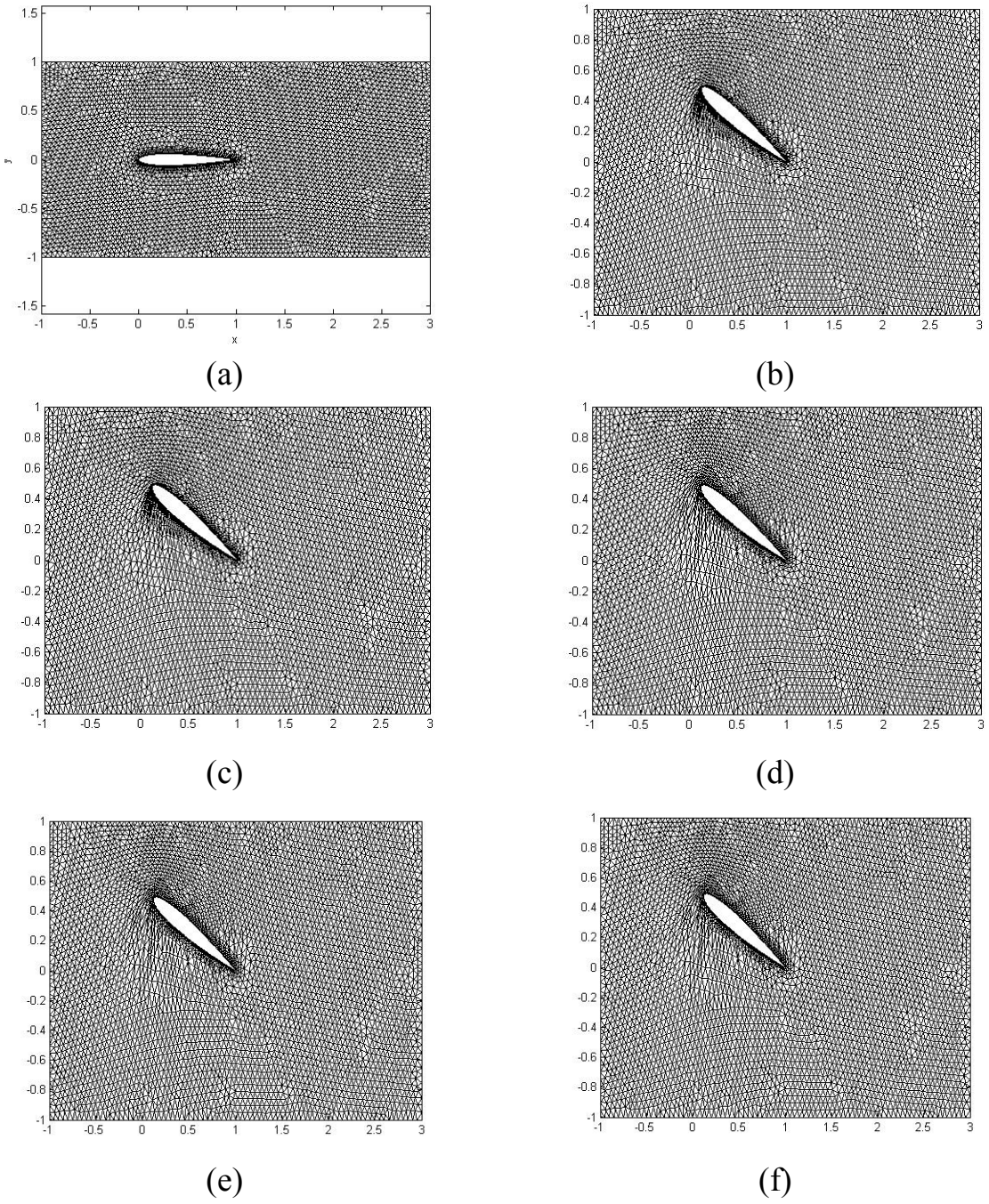

Fig. 1. Final configuration for different moving mesh methodologies

Figure 1 shows the undeformed, Fig. 1a, and deformed meshes, Fig. 1b to Fig. 1f, for each mesh moving methodology (Laplacian Fig. 1b, Lineal Springs Fig 1c, Torsional Springs Fig. 1d, Lineal-Torsional Springs Fig 1e and Pseudo-Stokes Fig. 1f). Each methodology moved the airfoil nodes to the same final angle of attack, about 30 degrees. One can note that the methods presented different forms of deformed elements at the surroundings of the airfoil, but some methodologies presented similar deformed mesh display. The Laplacian and

Lineal Springs methodologies presented a small number of flattened elements above the airfoil when compared with the remaining methodologies. Below the airfoil, the elements for the above mentioned methodologies appear less stretched than the remaining ones. The Torsional, Lineal-Torsional and Pseudo-Stokes methodologies show a higher number of flattened elements compared with the previous methodologies, with slightly more stretched elements below the airfoil.

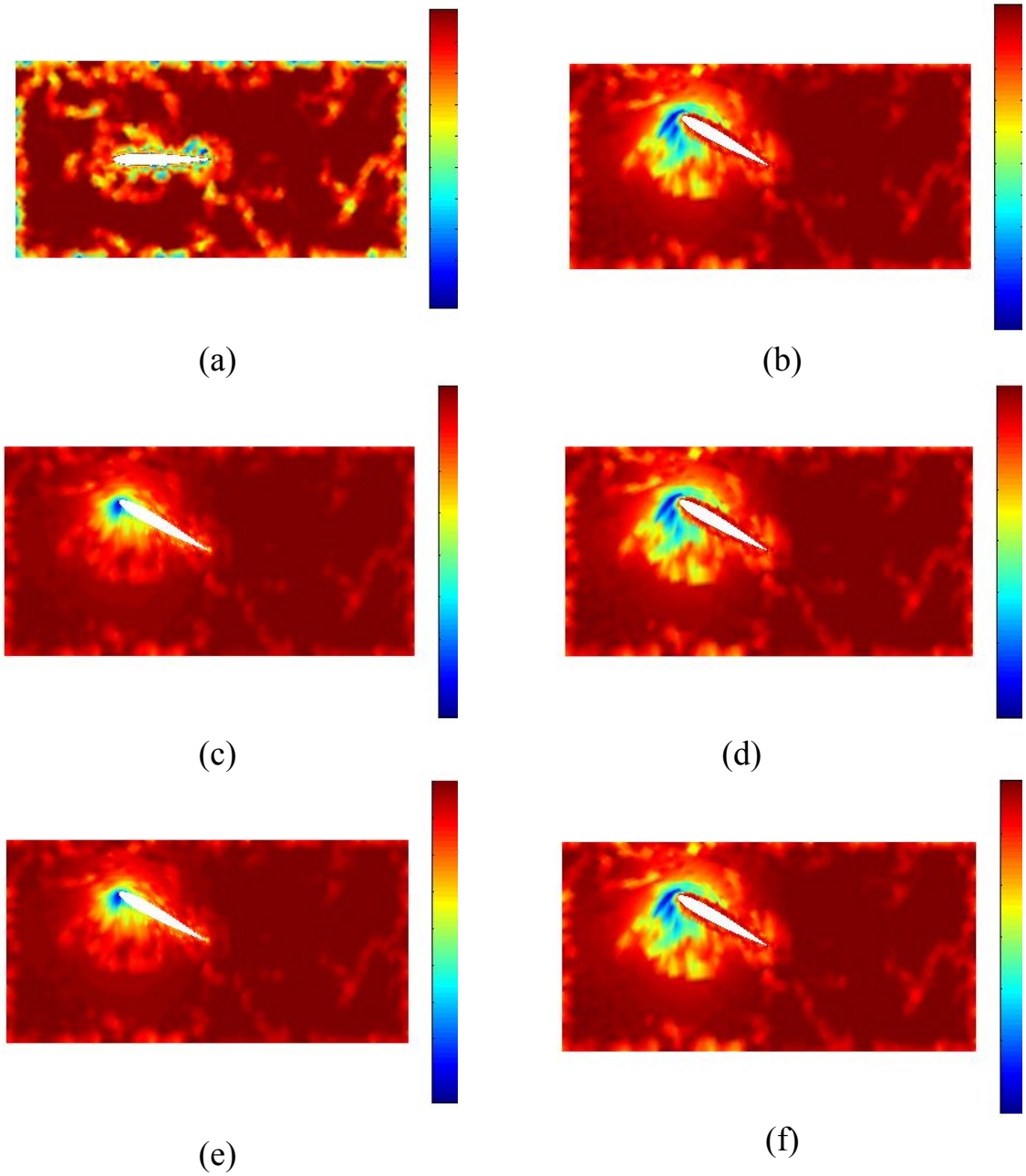

Fig. 2. Mesh quality for different moving mesh methodologies

Figure 2 shows the mesh quality parameter plotted for each element of the mesh for the undeformed mesh, Fig. 2a, and for the five methodologies, Fig. 2b to Fig. 2f (Laplacian Fig. 2b, Lineal Springs Fig 2c, Torsional Springs Fig. 2d,

Lineal-Torsional Springs Fig. 2e and Pseudo-Stokes Fig. 2f). The Lineal-Torsional and Lineal methods show elements with quality below 0.5 at the airfoil´s trailing edge. The Torsional, Laplacian, and Pseudo-Stokes methods presented elements with better quality at the same location. It is important to highlight that the fact that the leading edge elements that have a quality value below 0.5 does not mean that this element has poor quality geometry. As seen above, the quality values that will compromise the calculation are far below 1. So, a quality limit can be established. This limit will be determined by the effects caused by the mesh shape in the flow calculation. These effects will be noted by the flow results that will be generated with the deformed mesh. Further studies must be conducted to determine minimum quality values that ensure good flow calculation.

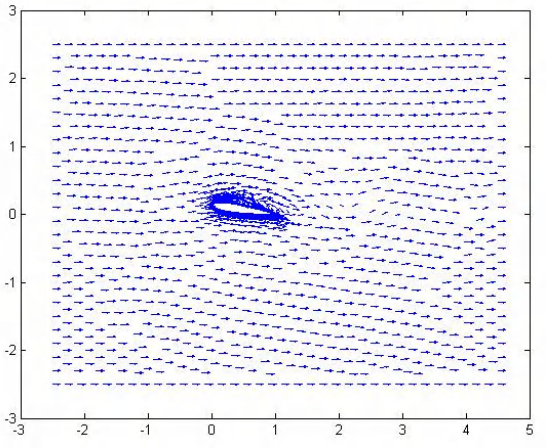

(a)

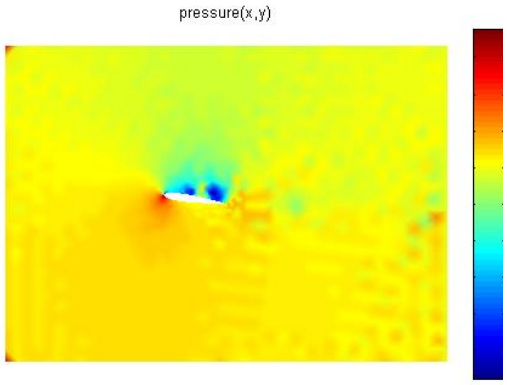

(b)

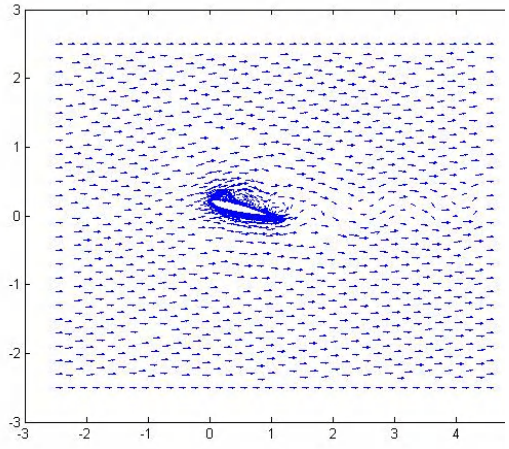

(c)

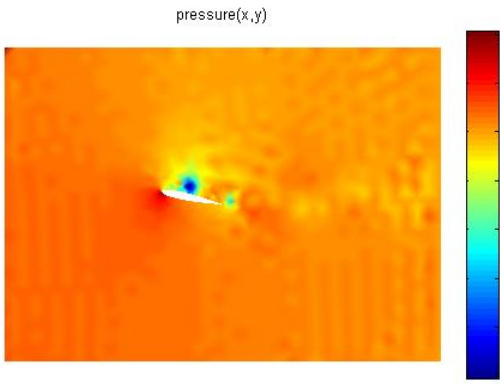

(d)

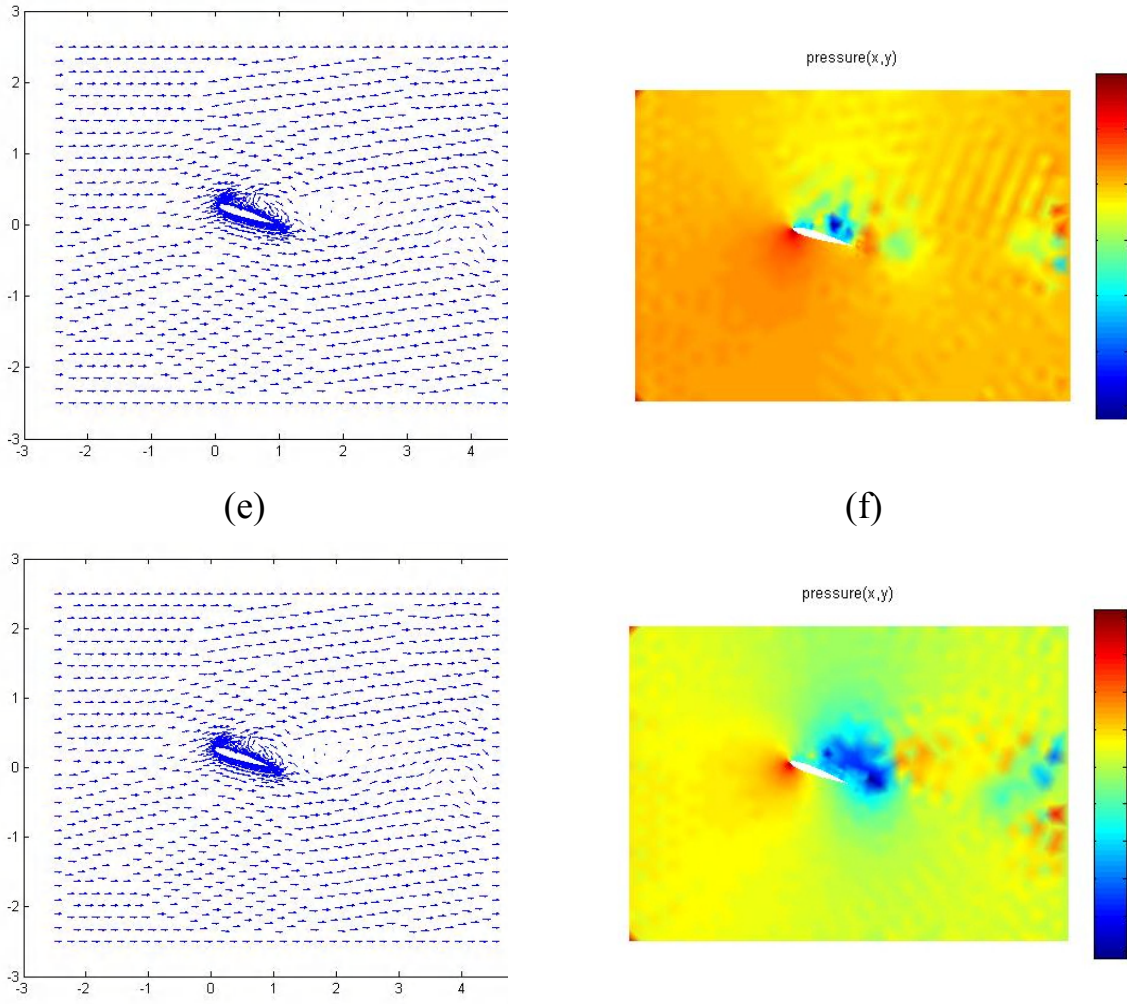

(e) (f)

(g) (h)

Fig. 3. Velocity Vectors and Pressure Contours (Lineal Torsional Springs)

The velocity vectors and pressure contours showed in Fig. 3a and 3b for 8 degrees, Fig. 3c and 3d for 12 degrees, Fig. 3e and 3f for 16 degrees, Fig. 3g and Fig. 3h for 20 degrees, respectively, show the dynamic stall pattern, Barcelos, Noleto e Brasil Junior (2009). The flow topology bears close similarity with the visualization results displayed at Naudascher and Rockwell (2005) and Svacek et al. (2007). In a pitching airfoil condition where the angle of attack increases, the boundary layer is fully attached at the lower surface of the airfoil, while the upper surface shows that the separation point moves upstream (figure 6). The presented flow topology is a free shear layer wake at the trailing edge, while the vorticity assumes a counterclockwise shedding pattern, which is consistent with the increasing airfoil circulation. One can note that on this phase of increasing angle of attack, the separation point remains moving upstream, until it reaches the leading edge, Digavallis (1993) and Fujisawa and Shibuya (2001). The shear layer at the upper surface rolls up, configuring the dynamic stall pattern, identified by a primary vortex formed. This vortex becomes bigger as it departs from the airfoil to, finally, detaches itself. At this moment, the shear layer that is

emitted from the trailing edge gains force, to generate the counterclockwise shedding mentioned before. At this moment, the normal force reaches its maximum value.

Conclusions

In this work several methodologies to solve the mesh motion problem were employed. Basically, two main strategies were chosen: Pseudo-Structural strategies, represented by the Laplacian, Lineal Springs, Torsional Springs and Lineal Torsional Springs, and Pseudo-Flow strategy, represented by the Pseudo-Stokes method. A quality parameter was used to evaluate the mesh after deformation, and the computational time was measured.

Results for all strategies had shown that all methodologies were able to move the mesh generated by an airfoil that increases its attack angle. The quality parameter analysis showed that the deformed meshes hold good quality for flow calculation. The visual results obtained for the deformed meshes show that the airfoil has moved to a position of 30 degrees with resulting final meshes that can provide robustness and stability for flow calculation. The main concern is regard to the computational time. All the Pseudo-Structural strategies has presented similar results, while the Pseudo-Stokes strategy demanded a small time step to ensure convergence and the condition of projection on a divergence-free space, and it has taken a high amount of computational time. Based on those results, one can conclude that the Pseudo-Structural strategies are better suited for flow calculation for the time being, while the Pseudo-Stokes strategy need more research to pose as an alternative to the remaining strategies.

Results of the numerical simulation of a laminar flow over a rotating NACA 0012 airfoil were presented, and those hold resemblance with experimental flow visualization available at the literature. Flow effects, such as vortex shedding, recirculation zones formation and shear layer shedding were observed.

References

1. Batina, J. T., 1990. Unsteady Euler airfoil solutions using unstructured dynamic meshes. AIAA Journal, vol. 28, n. 8, pp. 1381–1388.
2. Batina, J. T., 1991. Unsteady Euler algorithm with unstructured dynamic mesh for complex-aircraft aerodynamic analysis. AIAA Journal, vol. 29, n. 3, pp. 327–333.
3. Chorin, A. J., 1968. Numerical solution of the Navier-Stokes equations. Math. Compt., vol 22, pp. 745-762.
4. Codina, R., & Blasco, J., 2000. Stabilized finite element method for transient Navier-Stokes equations based on a pressure gradient projection. Comput. Methods Appl. Mech. Engrg., vol 182, pp. 277-300.

5. Codina, R., 2000. Pressure stability in fractional step finite element methods for incompressible flow. J. for Compt. Physics, vol. 170, pp. 112-140.
6. Degand, C., & Farhat, C., 2002. A three-dimensional torsional spring analogy method for unstructured dynamic meshes. Computers and Structures, vol. 80, pp. 305–316.
7. Digavalli, S., 1993. Dynamic Stall of a NACA 0012 in Laminar Flow, PhD thesis, Massachussetts Institute of Technology.
8. Farhat, C., Degand, C., Koobus, B., & Lesoinne, M., 1998. Torsinal springs for two dimensional dynamic unstructured fluid meshes. Comput. Methods Appl. Mech. Engrg., vol 163, pp. 231-245.
9. Fujisawa, N., Shibuya, S., 2001. Observations of dynamic stall on Darrieus wind turbine blades, Journal of Wind Engineering and Industrial Aerodynamics, vol. 89, pp. 201-214.
10. Goldberg, D., & Ruas, V., 1999. A numerical study of projection algorithms on finite element simulation of three-dimensional viscous incompressible flows. Int. J. Numer. Meth. Fluids, vol 30, pp. 233-256.
11. Guermod, J. L., Minev, P., & Shen, J., 2006. An overview of projection methods for incompressible flows. Comput. Methods Appl. Mech. Engrg., vol. 195, pp 6011-6045.
12. Jasak, H. & Tukovic, Z., 2007. Automatic mesh motion for the unstructured finite volume method. Transactions of FAMENA, vol. 30, n. 2, pp. 1-18.
13. Johnson, A. A., & Tezduyar, T. E., 1994. Mesh update stategies in parallel finite element computations of flow problems with moving boundaries and interfaces. Computer methods in applied mechanics and engineering, vol. 119, pp. 73–94.
14. Koobus, B., Farhat, C., Degand, C., & Lesoinne, M., 1998. An improved method of spring analogy for dynamic unstructured fluid meshes. In Proceedings of the 39th AIAA/ASME/ASCE/AHS/ASC structures, structural dynamics, and materials conference and exhibit, April 20-23, Long Beach, California.
15. Lohner, R., & Yang, C., 1996. Improved ALE mesh velocities for moving bodies. Communications in numerical methods in engineering, vol. 12, pp. 599–608.
16. Lohner, R., Yang, C., Cebral, J., Camelli, F. Soto, O., & Walts, J., 2006. Improving the speed and accuracy of the projection-type incompressible flow solvers. Comput. Methods Appl. Mech. Engrg., vol. 195, 3087-3109.
17. Massarotti, N., Arpino, F., Lewis, R. W., & Nithiarasu, P., 2006. Explicity and semi-implicit CBS procedures for incompressible viscous flows. International Journal for Numerical Methods in Engineering, vol. 66, pp. 1618-1640.
18. Naudascher, E. and Rockwell, D., 2005. Flow Induced Vibrations: An Engineering Guide. Dover.
19. Rypl, D., 1998. Sequential and parallel generation of unstructured 3D meshes. PhD thesis, Czech Technical University Reports.

20. Svacek, P., Feistauer, M., e Horacek, J., 2007. Numerical simulation of flow induced airfoil vibrations with large amplitudes. Journal of Fluids and Structures, vol. 23, pp. 391-411.
21. Noleto, L. G.; Barcelos, M.; Brasil Junior, A. C.P.. An Alternative Mesh Motion Methodology Based on a Pseudo-Stokes Problem. In: 30o. CILAMCE - Congresso Ibero-Americano de Métodos Computacionais em Engenharia, 2009, Búzios. Anais do 30º. CILAMCE - Congresso Ibero-Americano de Métodos Computacionais em Engenharia, 2009.
22. Barcelos, M.; Noleto, L. G.; Barcelos Junior, A. C.P.. A Finite Element Numerical Simulation of the Laminar Flow over an Oscillating Airfoil. In: 20th COBEM - International Congress of Mechanical Engineering, 2009, Gramado. Proceedings of 20th COBEM - International Congress of Mechanical Engineering, 2009.